Journal of Power Sources, *14* (1985) 223 - 229

CYCLING BEHAVIOUR OF MOLYBDENUM DICHALCOGENIDES IN APROTIC ORGANIC ELECTROLYTE SOLUTION

D. ILIĆ, K. WIESENER and W. SCHNEIDER

Dresden University of Technology, Department of Chemistry, Dresden (G.D.R.)

H. OPPERMANN and G. KRABBES

Academy of Sciences of the G.D.R., Central Institute of Solid State Physics and Materials Research, Dresden (G.D.R.)

Introduction

Layer structured transition metal chalcogenides are of special interest considering their application as positive active materials in high energy secondary cells with aprotic organic electrolyte solutions. Among the dichalcogenides of "two-dimensional" structure, titanium disulphide (TiS_2) has been most thoroughly investigated [1, 2]. However, various other substances of that type may be considered as electrodes [3]. Silbernagel [4], on the basis of NMR spectroscopic investigations of the intercalation of lithium into metal dichalcogenides of the MX_2 type with M = Mo, W, Sn, Re, and X = S, Se, postulated that intercalates of the formula Li_yMX_2 are produced as intermediates which subsequently are converted into Li_2X and metal M. The relation between the electronic and mechanical properties of the metal dichalcogenides and their structure has been described in numerous investigations [5, 6].

Experimental

The transition metal chalcogenides were made from the elements by direct synthesis in evacuated quartz glass ampoules at 800 °C for 96 h (Mo highly purified, less than 100 ppm impurities, freshly reduced with H_2; S twice sublimed; Se, Te superpure). MoS_2 shows the 2H-structure in addition to 3R-components; $MoSe_2$ also has the 2H-structure. α-$MoTe_2$ is also of 2H-type (with a small percentage of 3R-β-$MoTe_2$), whereas β-$MoTe_2$ shows the 3R-structure (with a small percentage of 2H-α-$MoTe_2$).

The cycling behaviour of MoS_2, $MoSe_2$, α-$MoTe_2$ and β-$MoTe_2$ in electrodes containing carbon black as a conductive material and Teflon as a binding agent was investigated in a glass cell having a lithium counter electrode, a lithium reference electrode, and an electrolyte solution of $LiClO_4$ (1 mol/l) in a propylene carbonate–dimethoxyethane solution (1:1).

0378-7753/85/$3.30

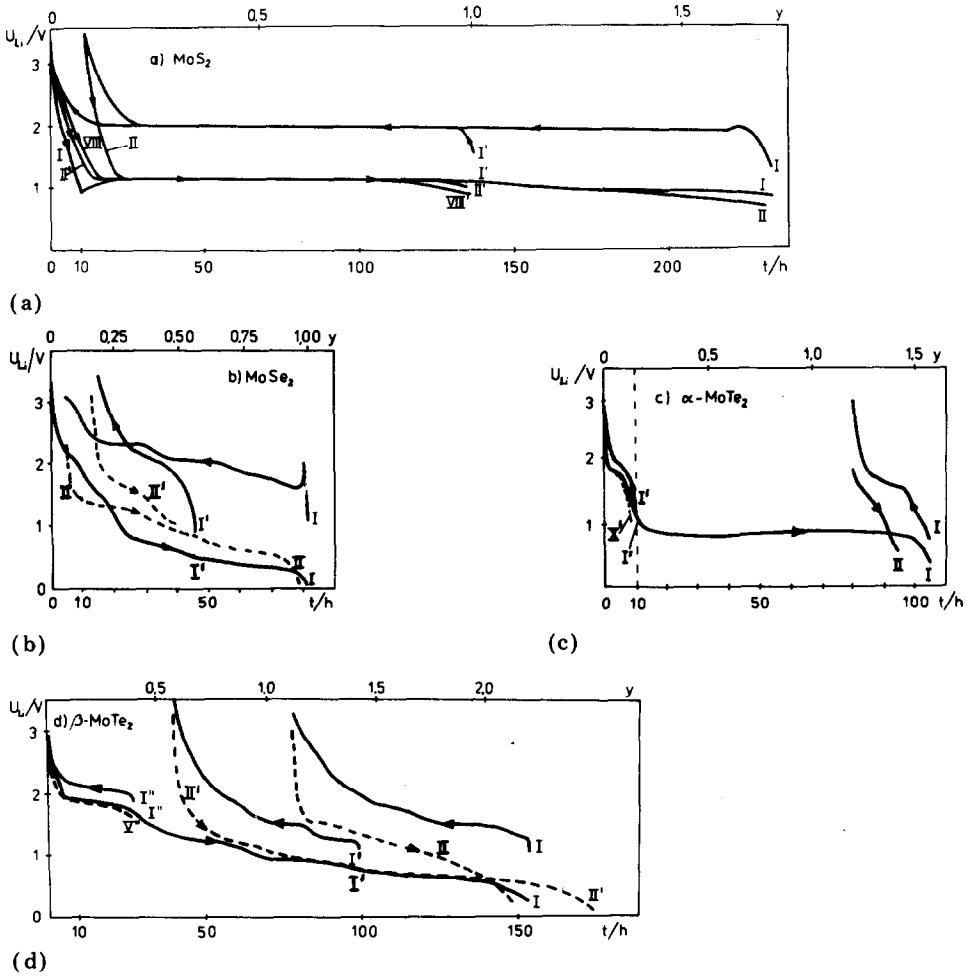

Fig. 1. Discharge–charge curve (0.3 mA/cm^2) of cells (a) Li–MoS_2, (b) Li–$MoSe_2$, (c) Li–α-$MoTe_2$, (d) Li–β-$MoTe_2$ in 1M $LiClO_4$ in propylene carbonate–dimethoxyethane (1:1); the charge curves are plotted from right to left; the Roman numerals indicate the cycle number.

Results and discussion

The results of the electrochemical measurements are represented in Figs. 1 and 2. It can be assumed that the electrochemical discharge reaction proceeds according to the following general equation:

$$yLi^+ + ye^- + MoX_2 \longrightarrow Li_yMoX_2 \qquad (1)$$

X = S, Se, Te

In Fig. 1 the discharge–charge curves for the first cycles are shown for MoS_2, $MoSe_2$, α-$MoTe_2$ and β-$MoTe_2$ in the above mentioned electrochemical

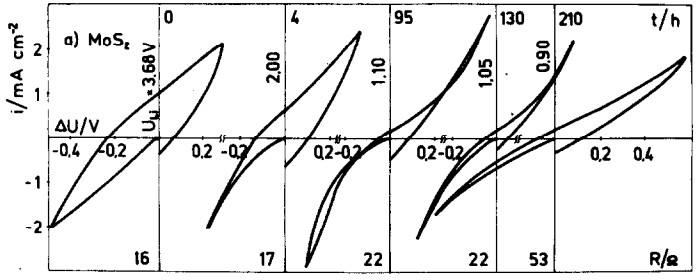

(a)

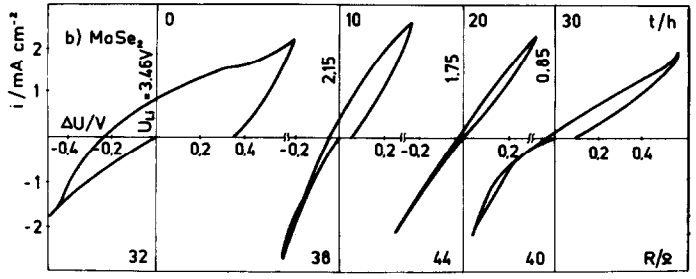

(b)

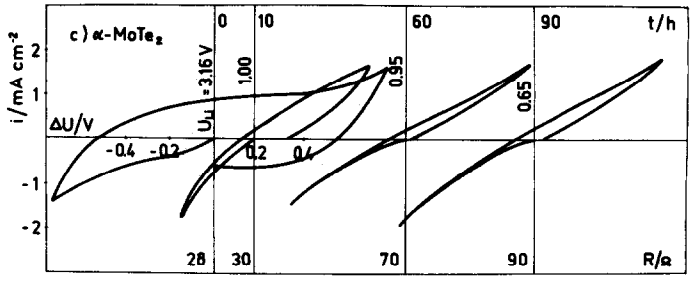

(c)

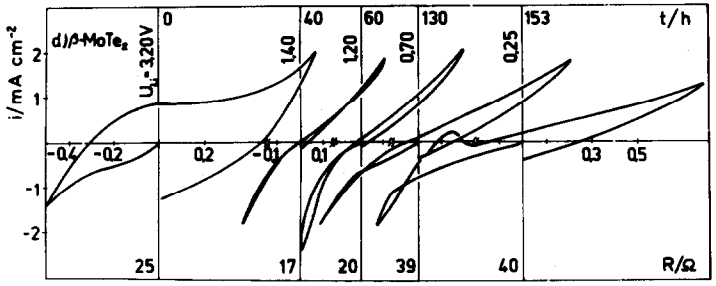

(d)

Fig. 2. Potentiodynamic potential–current density curves with ohmic voltage drop compensation of the first discharge of: (a) MoS_2, (b) $MoSe_2$, (c) α-$MoTe_2$, and (d) β-$MoTe_2$ in a lithium cell with 1M $LiClO_4$ in propylene carbonate–dimethoxyethane (1:1) solution.

system, with iR compensation, at the same discharge and charge current density of 300 $\mu A/cm^2$. The charge curves take a course opposite to the direction of the time axis (arrow from right to left). The Roman numerals on the curves indicate the number of the discharge–charge cycle. Where the loading process started at a lower depth of discharge the cycle numbers are indicated by one or two primes as an index.

Figure 2 shows the corresponding potentiodynamic potential–current density curves, with ohmic voltage drop compensation, of the first discharge, obtained at definite times of discharge. At each particular time which, in addition to the electrode potential U_{Li} and the ohmic resistance of the system, is given for each curve in Fig. 2, a potentiodynamic measurement was carried out. Here, the electrode was always polarized in the cathodic sense. By means of the potentiodynamic U_{Li}, i curves the reversibility of the cathodic and anodic processes can be determined. The closer together are the branches corresponding to increasing and decreasing polarization, the less the processes are retarded. The process is retarded to the greatest degree at the beginning of discharge ($y = 0$ in Li_yMoX_2). However, here also, as in most cases, the electrodes can be loaded to a current density of about 2 mA/cm^2; an increased polarization of about 0.6 V at approximately 1 mA/cm^2 occurs only in the case of α-$MoTe_2$ whereas, in all the others the polarisation is 0.2 - 0.3 V at this current density.

An extensive and nearly constant potential plateau at 1.0 - 1.2 V is found in the MoS_2 discharge curve (Fig. 1(a)), maintaining nearly the same value at discharge current densities up to 1 mA/cm^2. At higher current densities, however, a minimum voltage occurs as a result of the formation of Mo_6S_8 and the corresponding lithium intercalate, or of a phase transformation of the MoS_2, *i.e.*, of 3R to 2H. In Li_yMoS_2 the material can still be recharged at y values of 1.6. However, this behaviour is more definite at $y \leqslant 1.0$. Within the potential plateau the potentiodynamic potential–current density curves are of the same type (Fig. 2(a)) at practically the same ohmic resistance (22 Ω). At values of $y \geqslant 1.25$ the polarization increases; this becomes apparent as a considerable increase in the polarization resistance. The ohmic resistance also increases in the same direction.

The polarization properties of $MoSe_2$ under various discharge conditions are similar (Fig. 2(b)); a higher polarization of the electrode in the range $0 \leqslant y \leqslant 0.2$ is observed however. The discharge curve (Fig. 1(b)) at a y value of about 0.5 leads to a voltage plateau at less than 0.5 V. By comparing the Debye–Scherrer X-ray diffraction diagrams (Fig. 3) of the starting material, $MoSe_2$(2H), and the discharged product, the formation of the Li_yMoSe_2 phase is assumed. Even with $y = 1.1$, neither molybdenum nor lithium selenide was identified by X-ray diffraction. By contrast, Dey [7] who investigated the selenides of Cu, Fe, Ni, Mg and Pb as cathodic materials for lithium cells at voltage plateaux of 1.0 - 1.5 V found lithium selenide and the corresponding metal as the final products of the electrochemical reaction.

The considerable electrode polarization of α-$MoTe_2$ is reflected in the discharge curve (Fig. 1(c)), showing an evident decrease in the potential from

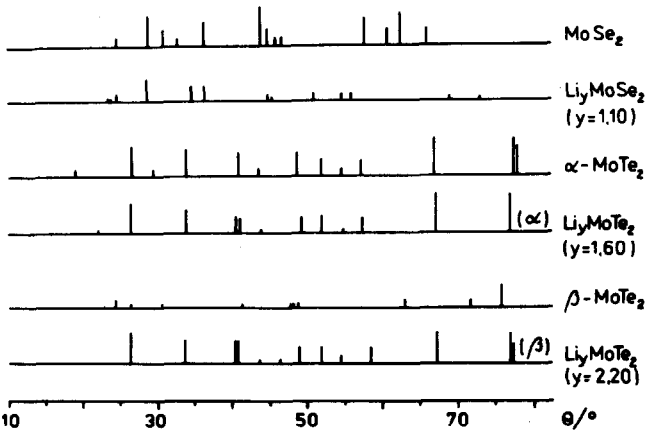

Fig. 3. X-ray diffraction diagrams of Debye–Scherrer patterns with Cr Kα radiation (V_2O_5 filter) for $MoSe_2$, α-$MoTe_2$ and β-$MoTe_2$ and for their discharge products in lithium cells.

the rest potential to 2.1 V and finally to about 1 V. At this potential, an extensive and stable plateau in the discharge characteristic exists, showing a slightly marked minimum at $0.5 < y < 0.6$. If the discharge is continued up to values of $y \geqslant 1.5$ the system can no longer be recharged.

Similar behaviour was observed by Dey [8] for the tellurides of Cu^{2+}, Ag^{+}, Pb^{2+}, Tl^{3+} and Bi^{3+}, and he recommended them for use as cathodic materials for electrochemical primary current sources.

It may be seen from the manner of the curves in Fig. 2(c) that with progressive discharge the ohmic resistance at $y > 0.2$ is increasing steeply. Up to this value ($y \leqslant 0.15$) the rechargeability is largely maintained, as can be seen by the cycle tests (Fig. 1(c)).

It is considered from the X-ray diffraction diagrams (Fig. 3) that, up to completion of discharge ($y = 1.6$), an intercalation of the lithium into the α-$MoTe_2$ structure takes place with the formation of $Li_yMoTe_2(\alpha)$. Molybdenum and lithium telluride were not identified.

In the discharge curve (Fig. 1(d)) for β-$MoTe_2$ several plateaux were observed, corresponding with y-value steps of about 0.5, 1.0 and 1.5. The cycle life decreases with increasing y-value. At $y \leqslant 1.4$ the system shows a sufficiently reversible behaviour which is especially evident at values of $y \leqslant 0.5$. For values of $y \geqslant 2$ the electrode cycle life is not so good.

This behaviour of β-$MoTe_2$ is also reflected in the potentiodynamic U_{Li}–i curves (Fig. 2(d)). With increasing y-value in Li_yMoTe_2, during discharge the polarization as well as the ohmic resistance increase. Whereas the electrode in the range $0.4 \leqslant y \leqslant 0.75$ shows a largely reversible behaviour, at values of $y \geqslant 1.6$ polarization and ohmic resistance increase considerably.

While molybdenum or lithium telluride are not identified in the discharged sample ($y = 2.2$) it is noticeable that with lithium incorporation into β-$MoTe_2$ the same phase arises as with α-$MoTe_2$.

The change in ohmic resistance during discharge is of special importance in regard to the discharge behaviour of the cells. The system's total resistance is the sum of the ohmic resistance, R_o, and of the polarization resistance, R_p:

$$R = R_o + R_p \tag{2}$$

In Fig. 4, the ohmic voltage drop of the lithium–molybdenum sulphide cell is plotted parallel to its discharge curve. At first its value increases, then remains constant at the voltage minimum and, during the transition into a second phase, increases until the discharge curve has reached the plateau value. During the further reduction of MoS_2 the ohmic resistance begins to increase again.

The change in the ohmic voltage drop during discharge of a lithium–molybdenum selenide cell is shown in parallel with its discharge curve in Fig. 5. The increase in the ohmic resistance is accompanied by all the changes occurring during the reduction of $MoSe_2$.

The results of the potentiodynamic investigations (Fig. 2) for different lithium contents (up to 1.5 equivalents per MoX_2) revealed that the behaviour during cycling depends on the lithium content and on the voltage sweep rate (optimum of the sweep rate is at 6.7 mV/s).

It is characteristic that a decrease in polarization occurs at the critical points of the discharge curves, and afterwards there is an increase. This is a result of the different bonding energies in the different intercalation steps and the controlled diffusion of the lithium in the matrix of the host lattice.

The electrochemical behaviour of the investigated chalcogenides is defined by their crystal structure as well as by their electronic structure. The influence of the hybrid orbitals (d_{z^2}) with the Fermi level, E_F, of about 1 eV,

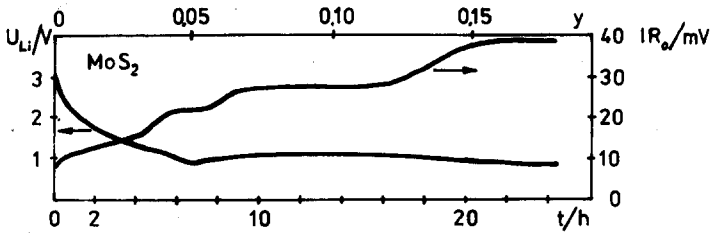

Fig. 4. Ohmic voltage drop curve and discharge curve (0.5 mA/cm^2) of an Li–MoS_2 cell with 1M $LiClO_4$ in propylene carbonate–dimethoxyethane (1:1).

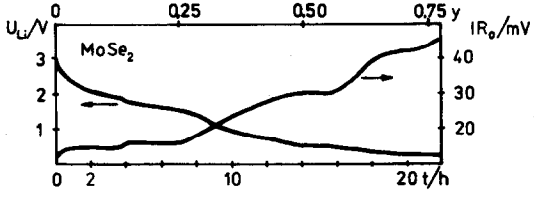

Fig. 5. Ohmic voltage drop curve and discharge curve (0.5 mA/cm^2) of an Li–$MoSe_2$ cell with 1M $LiClO_4$ in propylene carbonate–dimethoxyethane (1:1).

implying a trigonal bipyramidal crystal structure, is directly responsible for the possibility of the intercalation of lithium into the crystal matrix.

References

1 M. S. Whittingham, *Science, 192* (1976) 1126.
2 M. S. Whittingham and F. R. Gamble, *Mater. Res. Bull., 10* (1975) 363.
3 A. J. Jacobson, R. R. Chianelli and M. S. Whittingham, *J. Electrochem. Soc., 124* (1979) 2277.
4 B. G. Silbernagel, *Solid State Commmun., 17* (1975) 361.
5 J. A. Wilson and A. D. Yoffe, *Adv. Phys., 18* (1969) 183.
6 F. Jellinek, *Ark. Kemi, 20* (1963) 474.
7 A. N. Dey, *US Patent 3,681,144* (1972).
8 A. N. Dey, *US Patent 3,877,988* (1975).